

# Technical Notes

*TECHNICAL NOTES* are short manuscripts describing new developments or important results of a preliminary nature. These Notes should not exceed 2500 words (where a figure or table counts as 200 words). Following informal review by the Editors, they may be published within a few months of the date of receipt. Style requirements are the same as for regular contributions (see inside back cover).

## Iodine Tagging Velocimetry in a Mach 10 Wake

R. Jeffrey Balla\*

NASA Langley Research Center, Hampton, Virginia 23681

DOI: 10.2514/1.J052416

### Introduction

A variation on molecular tagging velocimetry (MTV) [1] designated iodine tagging velocimetry (ITV) is demonstrated. Molecular iodine is tagged by two-photon absorption using an Argon Fluoride (ArF) excimer laser. A single camera measures fluid displacement using atomic iodine emission at 206 nm.

Two examples of MTV for cold-flow measurements are N<sub>2</sub>O MTV [2] and Femtosecond Laser Electronic Excitation Tagging [3]. These, like most MTV methods, are designed for atmospheric pressure applications. Neither can be implemented at the low pressures (0.1–1 Torr) in typical hypersonic wakes. Of all the single-laser/single-camera MTV approaches, only Nitric-Oxide Planar Laser Induced Fluorescence-based MTV [4] has been successfully demonstrated in a Mach 10 wake. Oxygen quenching limits transit times to 500 ns and accuracy to typically 30%.

The present note describes the photophysics of the ITV method. Off-body velocimetry along a line is demonstrated in the aerothermodynamically important and experimentally challenging region of a hypersonic low-pressure near-wake in a Mach 10 air wind tunnel. Transit times up to 10  $\mu$ s are demonstrated with conservative errors of 10%.

### Method

Descriptions of the NASA Langley 31 in. Mach 10 (31M10) air wind tunnel and experimental setup have been presented [5,6]. Briefly, the 31M10 wind tunnel is operated at a single stagnation pressure ( $P_0 = 2.41$  Mpa/350 psi) and stagnation temperature ( $T_0 = 1000$  K/1350 °F). A 0.5% I<sub>2</sub>/N<sub>2</sub> mixture is seeded on the leeward backshell of a multipurpose crew vehicle (MPCV) model using a pressure tap. I<sub>2</sub> laser-induced fluorescence is excited along a 5.5 mm line using a broadband stable-resonator ArF excimer laser near 193 nm. Emission is monitored using a gated intensified charge-coupled-device (CCD) camera as the tagged region is displaced through space over transit times of 10  $\mu$ s. The laser is focused using an uncoated 600 mm focal length Suprasil lens. Focused laser energy is 2.5 mJ, focal spot size is  $\sim 200$   $\mu$ m, and Rayleigh length is  $\sim 65$  cm.

Received 30 October 2012; revision received 13 January 2013; accepted for publication 21 January 2013; published online 10 May 2013. This material is declared a work of the U.S. Government and is not subject to copyright protection in the United States. Copies of this paper may be made for personal or internal use, on condition that the copier pay the \$10.00 per-copy fee to the Copyright Clearance Center, Inc., 222 Rosewood Drive, Danvers, MA 01923; include the code 1533-385X/13 and \$10.00 in correspondence with the CCC.

\*Senior Research Scientist, Advanced Sensing and Optical Measurement Branch, MS 493; robert.j.balla@nasa.gov. Senior Member AIAA.

No interference filter is used. A composite image showing the model, iodine-seeded wake jet, laser beam, and velocity results can be found near the end of this note.

To examine the physics behind ITV, lab experiments were performed using an experimental setup with all laser characteristics and detectors identical to the wind-tunnel setup. A cell containing  $1 \times 10^{15}$  cm<sup>-3</sup> I<sub>2</sub> in 0.1 Torr air at 298 K was substituted for the wind tunnel. For spectrally resolved time-dependent emission studies, a spectrometer/photomultiplier tube replaced the gated CCD camera. For I<sub>2</sub> fluorescence imaging with increased optical collection, a home-built 4-in.-diam four-element lens replaced the 1 in. Nikon lens on the gated intensified CCD camera. The lens consists of four 100-mm-diam Suprasil-1 fused silica lenses with the following shape, focal length, center thickness, and lens-to-lens center spacing characteristics in millimeters: lens 1, biconvex: +150, 23, 30 mm; lens 2, plano-concave: -148, 2.97, 30 mm; lens 3, biconvex: +150, 23, 35 mm; and lens 4, plano convex: +250, 30 mm. Focal lengths are specified at 248 nm. A series of five apertures with inner diameters of 75, 75, 75, 60, and 32 mm were placed between each successive lens to reduce off-axis rays and improve resolution.

### Lab Results

The ITV mechanism is not fully understood. The term ITV is used to include the possibilities of both molecular and atomic tagged states. Figure 1a shows that molecular iodine excited by an ArF excimer laser produces long-lived atomic iodine emission at 206.16 nm from  $I^2P_{3/2} \rightarrow I^2P_{1/2}^0$ . No similar long-lived emission was observed as the spectrometer was tuned from 190 to 205 nm and from 207 to 400 nm.

Instantaneous images (200 ns shutter) in nonflowing iodine are shown in Figs. 2a–2d. Images are cropped to show only 7 mm (20%) of the imaged line. Emission is observed using a 25-mm-diam aperture Nikkor lens and CCD camera delay times from the laser pulse of 0.2, 2, 5, and 10  $\mu$ s. Averaged images (371 single shots) using the 100-mm-diam aperture home-built lens and CCD camera delay times of 20 and 30  $\mu$ s are shown in Figs. 2e and 2f. The signal-to-noise ratio is  $\sim 6$  and  $\sim 3$  in Figs. 2e and 2f, respectively. Signal levels between Figs. 2a and 2f decrease by  $\sim 6400\times$ .

Instantaneous images show a transition from spatially uniform emission (Fig. 2a) at short delay times to spatially localized non-uniform emission (Figs. 2c and 2d) at longer delay times. All emission is observed at 206 nm. The spatially localized nonuniform emission at long delay times is a result of low photon statistics at long delay times ( $<10$  photoelectrons per pixel), detector gain at the maximum setting, and a nonadjustable mismatch between the dc levels of the CCD camera and digitizer, producing a negative baseline.

Energy requirements for 206 nm emission dictate at least a two-photon absorption process. Martin et al. [7] provided evidence for the latter near 193 nm along with significant amounts of ions ( $\sim 10^{12}$  cm<sup>-3</sup>) and therefore electrons. Given an I<sub>2</sub> ionization energy of 9.3074 eV [8], a 193 nm two-photon absorption process has 12.83 eV and will ionize I<sub>2</sub>. At these energy levels, I<sub>2</sub><sup>+</sup>, I<sup>+</sup>, and I<sup>-</sup>, “hot” electrons and thermal electrons can be produced [9]. Because no known radiative properties of neutral or ionic iodine atoms or molecules can produce the long-lived emission in Figs. 1 and 2, attention is given to chemical processes. They must be capable of storing energy for  $>10$   $\mu$ s and releasing it via a mechanism that

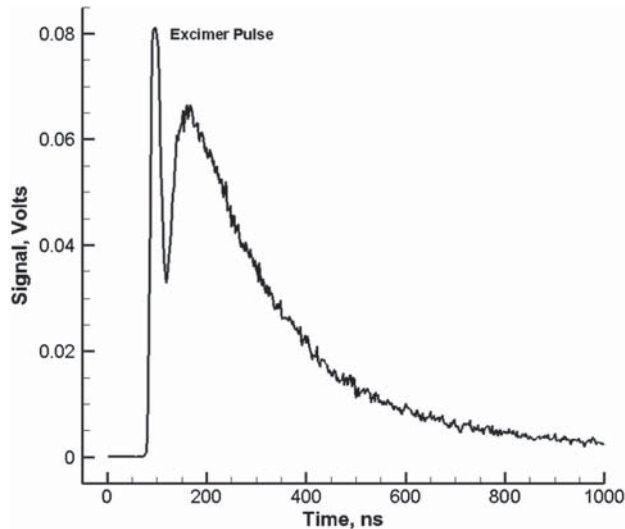
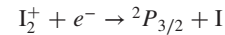


Fig. 1 Atomic iodine emission at 206.16 nm vs time.

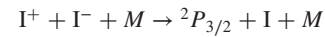
produces 206 nm emission. Possibilities based on exothermic thermochemical considerations are given in reactions 1–3. I refers to a ground electronic state iodine atom, and  $I^{**}$  refers to a highly electronically excited iodine atom. For both I and  $I^{**}$ , the energy levels are not specified.  $M$  represents a buffer gas that can remove excess energy by collisions. Reactions 1 and 3 represent electron–ion recombination. Reaction 2 represents ion–ion neutralization. Hemmati and Collins [10] favor reaction 1, while Barnes and

Kushnera [11] favor reaction 2. The literature contains iodine energy-level diagrams to aid the reader [10,11]. Further research is required to identify the reaction responsible for ITV emission.

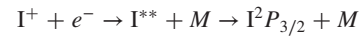
Reaction 1:



Reaction 2:



Reaction 3:



### Wind-Tunnel Results

The first demonstration of ITV is shown in Fig. 3. This approach monitors  $I^2P_{3/2} \rightarrow I^2P_{1/2}^0$  emission at 206 nm in the near-wake of an MPCV model (Fig. 4). Fluid conditions at the locations probed in the  $I_2/N_2$  jet in Fig. 4 are 300–400 K,  $0.13 \times 10^{17} \text{ cm}^{-3} N_2$ , and 0.42 Torr air [5].  $I_2$  jet density ( $2.5 \times 10^{14} \text{ cm}^{-3}$ ) is two orders of magnitude below the  $I_2$  vapor pressure. Figure 3a is the composite of three separate time-averaged images, one showing ITV start position using Rayleigh scattering and two showing ITV time-averaged downstream iodine fluid transit times of 5 and 10  $\mu\text{s}$ . Images at these transit times are readily achieved by combining the CCD camera gating and variable-gain capabilities. Each of the three images in Fig. 3a is the average of 371 instantaneous images. The instantaneous image in Fig. 3b shows spatially localized iodine emission similar to lab results observed in Fig. 2 at delay times beyond 2  $\mu\text{s}$ . Figure 3c

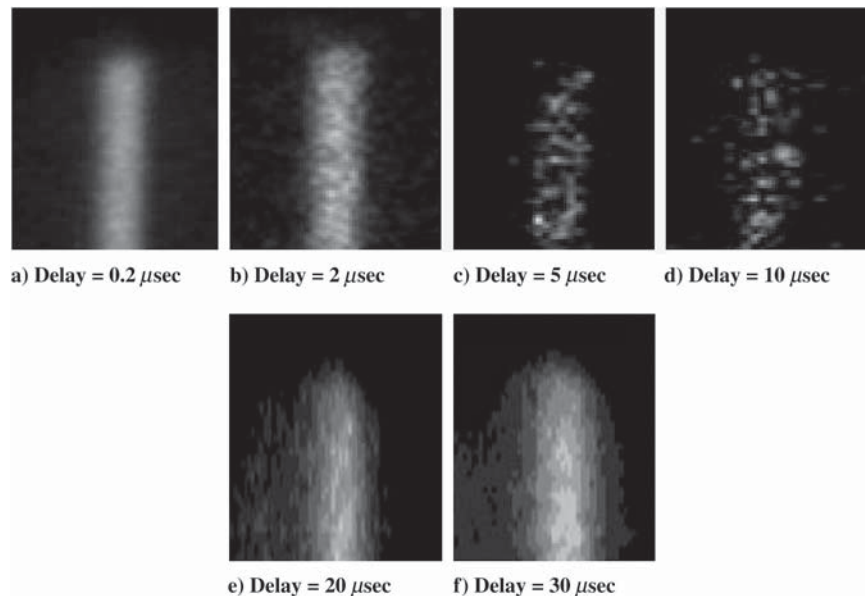


Fig. 2 Laboratory iodine fluorescence time-delayed images: a–d) single-shot images using 25 mm aperture Nikon lens, and e–f) average images using 100 mm aperture lens.

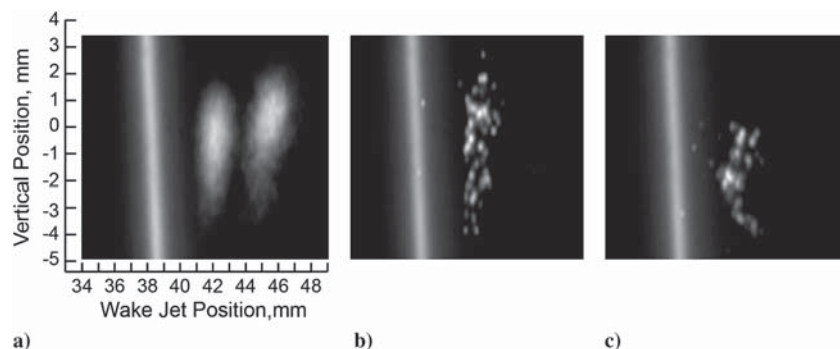


Fig. 3 Iodine tagging velocimetry: a) time-averaged composite images at 0, 5, and 10  $\mu\text{s}$  transit times, and b–c) instantaneous images at 5  $\mu\text{s}$  transit times.

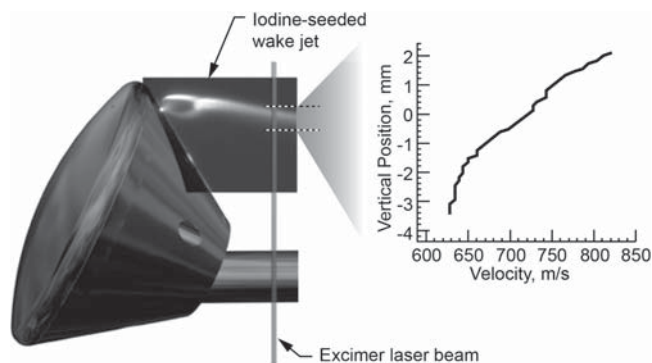


Fig. 4 ITV in a Mach 10 wake.

demonstrates the capability of ITV to measure the instantaneous spatial variation of the tagged fluid in location and shape. The 0 mm vertical and wake jet positions are keyed to the pressure tap in Fig. 4 where  $I_2$  is seeded.

A composite image showing the model, iodine-seeded wake jet [5], laser-beam location, and average velocity results from Fig. 3a at 10  $\mu$ s transit time are shown in Fig. 4. Velocities are normal to the exciting laser beam at 44 points along a 5.5 mm line. The transverse velocity component is not measured. Velocities vary from 630 to 820 m/s (30%) and increase toward the shear layer. Errors are estimated conservatively at 10%. Extrapolation of Fig. 4 results suggests that gas velocity within and beyond the shear layer is  $>820$  m/s or  $>59\%$  of freestream velocity. Because the wake jet gas temperature is  $\sim 300$  K [5], the jet Mach number varies from  $\sim 1.9$  to  $\sim 2.4$  across Fig. 4.

### Conclusions

The first demonstration of time-of-flight-based iodine tagging velocimetry (ITV) is presented. Transit times up to 10  $\mu$ s are observed. ITV is well suited for spatially resolved velocimetry measurements to study the fundamental flow physics of cold-flow hypersonic near and far wakes. ITV has the added advantage of simplicity through use of a single laser and camera. Additional research is required to identify the reaction mechanism, to understand all subtleties of this process, and to determine if there are other emission pathways that can be used for velocimetry.

### Acknowledgments

The author thanks Mark Kulick for aiding instrumentation assembly as well as R. J. Exton and Joel Tellinghuisen for many helpful comments.

### References

- [1] Koochesfahani, M. M., and Nocera, D. G., "Molecular Tagging Velocimetry," *Handbook of Experimental Fluid Dynamics*, edited by Foss, J., Tropea, C., and Yarin, A., Springer-Verlag, Berlin, 2007, Chap. 5.4.
- [2] ElBaz, A. M., and Pitz, R. W., "N<sub>2</sub>O Molecular Tagging Velocimetry," *Applied Physics B*, Vol. 106, No. 4, 2012, pp. 961–969. doi:10.1007/s00340-012-4872-5
- [3] Michael, J. B., Edwards, M. R., Dogariu, A., and Miles, R. B., "Femtosecond Laser Electronic Excitation Tagging for Quantitative Velocity Imaging in Air," *Applied Optics*, Vol. 50, No. 26, 2011, pp. 5158–5162. doi:10.1364/AO.50.005158
- [4] Bathel, B. F., Danehy, P. M., Inman, J. A., Jones, S. B., Ivey, C. B., and Goynes, C. P., "Velocity Profile Measurements in Hypersonic Flows Using Sequentially Imaged Fluorescence-Based Molecular Tagging," *AIAA Journal*, Vol. 49, No. 9, 2011, pp. 1883–1896. doi:10.2514/1.J050722
- [5] Balla, R. J., and Everhart, J. L., "Air Density Measurements in a Mach 10 Wake Using Iodine Cordes Bands," *AIAA Journal*, Vol. 50, No. 6, 2012, pp. 1388–1397. doi:10.2514/1.J051523
- [6] Balla, R. J., and Everhart, J. L., "Rayleigh Scattering Density Measurements, Cluster Theory, and Nucleation Calculations at Mach 10," *AIAA Journal*, Vol. 50, No. 3, 2012, pp. 698–707. doi:10.2514/1.J051334
- [7] Martin, M., Fotakis, C., Donovan, R. J., and Shaw, M. J., "Optical Pumping and Collisional Quenching of  $I_2 D^1 \Sigma_u^+$ ," *Nuovo Cimento B*, Vol. 63, No. 1, 1981, pp. 300–308. doi:10.1007/BF02721437
- [8] Cornford, A. B., Frost, D. C., McDowell, C. A., Ragle, J. L., and Stenhouse, I. A., "Photoelectron Spectra of the Halogens," *Journal of Chemical Physics*, Vol. 54, No. 6, 1971, pp. 2651–2657. doi:10.1063/1.1675227
- [9] Hewitt, S. A., Zhu, L., and Flynn, G. W., "Diode Laser Probing of CO<sub>2</sub> and CO Vibrational Excitation Produced by Collisions with High Energy Electrons from 193 nm Laser Photolysis of Iodine," *Journal of Chemical Physics*, Vol. 97, No. 9, 1992, pp. 6396–6409. doi:10.1063/1.463700
- [10] Hemmati, H., and Collins, G. J., "Laser Excited Fluorescence of  $I_2$ ," *Chemical Physics Letters*, Vol. 75, No. 3, 1980, pp. 488–493. doi:10.1016/0009-2614(80)80561-6
- [11] Barnes, P. N., and Kushnera, M. J., "Ion–Ion Neutralization of Iodine in Radio-Frequency Inductive Discharges of Xe and I<sub>2</sub> Mixtures," *Journal of Applied Physics*, Vol. 82, No. 5, 1997, pp. 2150–2155. doi:10.1063/1.366022

R. Lucht  
Associate Editor